THE INTERNAL BLAST WAVE PRODUCED IN A
CLOSED RANGE BY A 155mm HOWITZER GUN

Y. Kivity, RAFAEL Ballistics Center, Haifa, Israel.

and

D. Palan, PALAN CONSULTING ENGINEERS, Luxembourg.

ABSTRACT

This work is concerned with the internal air blast resulting from firing a
155mm Howitzer gun in a closed test range. The range is about 260 meters long
and has a typical cross-section of 5x6 meters. Various openings in the range
are closed by steel doors. A good estimate of the dynamic load on the doors
is critical for their proper design, and is the main objective of the present
study.

The pressure loading on the walls is calculated using a numerical hydro-
dynamic code. The problem is formulated as a quasi one-dimensional flow in a
variable area duct. The initial conditions of the flow at the muzzle gun
position are derived from a simplified model for the mixing of the hot
combustion products of the propellant and a finite mass of the ambient air.
In addition, two-dimensional calculations were carried out to get more
detailed distributions of the pressure loading at the target end and at the
firing arena. It is found that reflected overpressure levels of about 35 KPa
(≈5 psi) are attained for typical periods of about 100 ms.

	Form Approved OMB No. 0704-0188

Report Documentation Page

1. REPORT DATE **AUG 1990**	2. REPORT TYPE	3. DATES COVERED **00-00-1990 to 00-00-1990**
4. TITLE AND SUBTITLE **The Internal Blast Wave Produced in a Closed Range by a 155mm Howitzer Gun**		5a. CONTRACT NUMBER
		5b. GRANT NUMBER
		5c. PROGRAM ELEMENT NUMBER
6. AUTHOR(S)		5d. PROJECT NUMBER
		5e. TASK NUMBER
		5f. WORK UNIT NUMBER
7. PERFORMING ORGANIZATION NAME(S) AND ADDRESS(ES) **RAFAEL Ballistics Center, ,Haifa, Israel,**		8. PERFORMING ORGANIZATION REPORT NUMBER
9. SPONSORING/MONITORING AGENCY NAME(S) AND ADDRESS(ES)		10. SPONSOR/MONITOR'S ACRONYM(S)
		11. SPONSOR/MONITOR'S REPORT NUMBER(S)

12. DISTRIBUTION/AVAILABILITY STATEMENT
Approved for public release; distribution unlimited

13. SUPPLEMENTARY NOTES
See also ADA235005, Volume 1. Minutes of the Explosives Safety Seminar (24th) Held in St. Louis, MO on 28-30 August 1990.

14. ABSTRACT
see report

15. SUBJECT TERMS

16. SECURITY CLASSIFICATION OF:			17. LIMITATION OF ABSTRACT	18. NUMBER OF PAGES	19a. NAME OF RESPONSIBLE PERSON
a. REPORT **unclassified**	b. ABSTRACT **unclassified**	c. THIS PAGE **unclassified**	**Same as Report (SAR)**	**22**	

Standard Form 298 (Rev. 8-98)
Prescribed by ANSI Std Z39-18

1. INTRODUCTION

Safe testing of large caliber guns and ammunition in the open field requires a large area to be closed as a precaution against the various hazards associated with the firing. An alternative approach would be to conduct the testing within a closed structure. Such a structure will have to withstand the dynamic blast loading generated by the gun. In particular, the loading on various doors in the structure is required as an input for their design.

The present paper deals with the internal blast loading generated in a closed firing range by a 155mm Howitzer gun. The main structure of the range is essentially a long tunnel extending for about 260m, with internal cross-sectional dimensions of 5m wide and 6m high. The range includes two firing chambers along the tunnel, having slightly larger cross-sections, and a target chamber which is designed to contain all possible effects of rounds hitting the target or chamber.

The blast wave produced in a closed structure due to an energy burst is significantly different from the blast wave in a free air, when long times are considered. This is so because the walls of the structure reflect the incident wave, and thus contain the energy to a confined space. As a result the pressure levels and impulses in a closed structure may be much higher than the corresponding ones for the free blast wave.

In the closed proof range described above the energy containment effect is even more severe due to the tunnel-like geometry of the structure. This geometry forces the blast wave to move in one direction, thus focussing the momentum of the blast in the longitudinal direction. As a result, the decay of blast peak pressure with distance is much slower than in the spherical case. Baker [1] quotes Lindberg and Firth who studied blast wave propagation for three different symmetries: plane, cylindrical, and spherical. The results show very clearly that in the region where the spherical wave decays with the third power of distance, the plane wave decays only with the first power.

In the present work, the blast wave propagation is calculated using the hydrodynamic computer code SCALE. This code can handle a time dependent two-dimensional compressible flow and its dynamic interaction with a thin shell structure. In the present case, due to the elongated shape of the proof range, a quasi one-dimensional approximation was found adequate for studying the gross behavior of the blast. To get more details of the loading on the target end, a full two-dimensional model was employed. Examples of detailed calculations for blast waves from high explosive charges may be found in references [2] and [3].

The paper includes several preparatory sections to establish the validity of the calculations. Section 2 describes the model for the initial muzzle blast. Section 3 gives the details of the numerical solution. Section 4 discusses the propagation of a blast wave in a long tunnel. A parametric study of the initial muzzle blast effect on the wall load is given in section 5, and the convergence of the numerical scheme is demonstrated in section 6.

Sections 7-10 deal with the loading on the doors. Section 7 gives the one-dimensional solution for a variable cross section range, with emphasis on the target end. In Section 8 a more detailed two-dimensional calculation for the target end is given. In Section 9 the load on the firing chamber door is obtained. Finally, Section 10 treats the effect of venting from the firing chamber door, simulating a firing with an open door.

2. MUZZLE BLAST MIXING MODEL

Following the exit of the projectile from the muzzle, the hot combustion products of the propellant eject out in the form of an energetic stream which mixes with a large mass of the ambient air. The mixing process is very complex, and its determination would require significant computational and experimental efforts [4]. In the present investigation, however, we are interested in the flow at large distances from the mixing region, and therefore it suffices to consider only an average state of the mixing region. The averaged flow variables of the mixture will serve as initial conditions for the blast wave calculation.

It will be assumed that the total energy of the propellant E is divided into three main parts: Kinetic energy of the projectile, Kp, kinetic energy of the combustion gases, Kc, and internal energy of the combustion products, Uc, so that

$$E = Kp + Kc + Uc$$

In the above energy balance several energy losses were neglected, namely, frictional losses to the barrel, heat losses to the barrel and projectile, and other minor losses such as energy needed for spinning the projectile. All these losses are included in U, in order to obtain a conservative estimate of the blast energy. For convenience, the kinetic energy components will be represented as fractions of the total propellant energy:

$$Fp = Kp/E \ , \ \ Fc = Kc/E$$

The combustion products are assumed to mix with a finite volume of the ambient air, V, such that the internal energy and momentum of the mixture are conserved in the process. This results in the following relations for the mixture average properties:

$$M = Mc + Ma \ \ ; \ \ d = M/V$$

$$U = Uc + Ua \ \ ; \ \ e = U/M$$

$$W = Mc/M \ Wc \ \ ; \ \ Kc = \tfrac{1}{2} \ Mc \ Wc^2$$

Here M,U and W are the mixture mass, internal energy and velocity, respectively; d and e are the density and specific internal energy of the mixture. The pressure is determined by d and e using the equation of state (ideal gas, with specific heat ratio equal to that of air). The indices c and a refer to combustion products and air, respectively.

For a given propellant mass and energy, one has to specify Fp, Fc and the air volume V in order to close the model. Krier and Adams [5] give a typical energy balance for large caliber guns, which shows that Fp is around 0.32. Fc is more difficult to estimate, since the kinetic energy of the gases leaving the barrel varies with time. A representative average value of this velocity is the projectile velocity. Assuming that the combustion products have a uniform velocity enables to determine Fc. As an example, assume a propellant mass of Mc=10Kg, combustion products velocity Wc = 1000 m/s, the kinetic energy Kc is then ~5 MJ. To detrmine the total propellant energy one needs the propellant specific energy Q. Reference [6] gives typical values of the propellant impetus in the range F=1.0-1.1 MJ/Kg. To be on the safe side, the larger value of 1.1 MJ/Kg is adopted. The specific energy of the propellant Q is found from the relation [7]

$$Q = F/(\tau - 1)$$

Here τ is the ratio of specific heats of the combustion products. For the 155mm charge $\tau=1.24$. Therefore:

$$Q \sim 4.6 \text{ MJ/Kg}$$
$$E = Mc \ Q = 46 \text{ MJ}$$
$$Fc = Kc/E \sim 0.11$$

The remaining parameter in the model is the volume of the air that mixes with the combustion products. It will be assumed that V is the volume of the cell in the computational mesh that represents the muzzle region. The actual value depends on the particular choice of the mesh. In the uniform cross-section study V was in the range 40-60 cubic meters. In the variable cross-section V was about 100-250 cubic meters.

3. NUMRERICAL SOLUTION

The hydrodynamic calculation was carried out using the computer program SCALE. This program is based on numerical schemes employed in well known hydrocodes such as SALE [8], DISCO [9] and PISCES [10]. The air was represented as an ideal gas with a specific heat ratio of 1.4. For the preliminary study of the uniform cross-section range, the computational mesh consisted of a column of equally spaced grid points, representing a column of air in the tunnel-like range. The length of this column was divided to 70 cells of 3.33 m each. The air is assumed to be initially at standard conditions and at rest, except in one cell which represents the muzzle blast field. In that cell, the initial conditions of density, pressure and material velocity were taken according to the mixing model which was described in the previous section. The boundary conditions were taken as rigid wall at both ends of the column.

4. UNIFORM CROSS-SECTION RANGE

The uniform cross-section range is regarded as a simple model for studying the main features of the blast waves. The main tunnel section of the proof range, with a cross-section of 5x6 meters, is represented as a circular tube with a radius of 3.09 m. (Fig.1). The tube is 235 meter long, with the target end at the Z=-200 m coordinate, and the firing chamber door at Z=+35. The gun muzzle is located at the origin (Z=0). For this case the entire energy of a 10 Kg propellant was assumed to be converted to internal energy of the combustion products (Fc=Fp=0).

The blast field evolution in time is shown in Figs.2-7 by the pressure distributions in the tube, and by pressure time histories at two locations, Figs.8-9. All the figures show overpressure normalized by standard atmospheric pressure.

At t=0 the high pressure at Z=0 gives rise to two shock waves moving in opposite directions away from Z=0. The backward facing shock (i.e. the wave moving towards the firing chamber door) hits the door at t≈75 ms, and is amplified due to reflection at the closed end. Fig.2 shows clearly the reflected shock with an overpressure of about 0.75. At the same time the wave facing the target end has progressed about 35 m and has an amplitude of about 0.37. At t=200 ms (Fig.3), both waves have progressed further towards the target, while their amplitude has decayed to about 0.25. Fig.4 shows the distribution at t=550 ms, when the leading shock has just hit the target end. Due to reflection, the leading shock amplitude is about 0.4, or about twice that of the shock behind it. Fig.5, at t=800 ms, shows the two reflected waves now moving back towards the firing chamber, with an amplitude of ≈0.15. Subsequent distributions show the waves moving further, with some more decay of their peaks (Fig.6, t=1150 ms), and after reflection from the firing chamber end (Fig.7, t=1500 ms).

Figs.8-9 show pressure time histories at two locations. Fig.8 gives the pressure at the firing chamber door. The backward shock wave arrives at t≈40 ms and reaches its peak due to reflection at t≈75 ms. The finite rise time is a result of the numerical scheme which smears the shock discontinuity over a finite number of grid cells. The overpressure remains close to zero until the arrival of the two shock waves (described earlier) after reflection from the target end (t≈1150 ms). A more interesting pressure time history is shown in Fig.9 for the target end. It shows two peaks, amplified by reflection to an amplitude of about 0.4.

5. EFFECT OF MIXING MODEL PARAMETERS

The mixing model of section 4 assumes that the momentum of the combustion products is imparted to the entire mixture. Although this is a plausible assumption in the average sense, its accuracy can not be taken forgranted. Since an accurate description of the mixing process is outside the scope of the present work, a short parametric study of the effect is given.

For the parametric study the following values are assumed:

Total propellant energy: $E = 46$ MJ
Projectile kinetic energy fraction: $Fp = 0.30$
Volume of air in the mixture: $V = 60$ cu.m.

Four cases were calculated, with $Fc = 0$, 0.1, 0.2 and 0.6. The results of these calculations are summarized in Table 1. Fig.10 shows the overpressure time history at the target end for $Fc=0$. The peaks are 0.33 and 0.29. These values are lower than those of Fig.9 since in the present case with $Fp=0.3$ there is less energy available to the mixture. The following Fig.11 for the extreme value of $Fc=0.6$ shows a consistent trend of an increase in the first peak and a decrease in the second peak. The sum of the two peaks is almost constant, as is evident from Table 1.

TABLE 1
Peaks of the Normalized Overpressure as Function
of the Combustion Products Kinetic Energy

Fc	First Peak	Second Peak	Sum
0	0.33	0.29	0.62
0.1	0.37	0.25	0.62
0.2	0.39	0.24	0.63
0.6	0.42	0.15	0.57

It may be concluded from these results that the gas kinetic energy may increase the peak pressure by about 27%. In section 2, Fc was estimated as 0.11. One may take $Fc=0.1$ as a working approximation and expect the model variation to be within ±13% of the calculated figure.

6. NUMERICAL CONVERGENCE

The numerical scheme used in the SCALE code employs the artificial viscosity method for treating shock wave discontinuities in the flow. As a result both shock level and steepness depend on the mesh size. The numerical results presented above were obtained for a mesh of 70 cells. A question arises as to how far are these results from the theoretical limit of the solution when the number of cells is very large.

To test the convergence of the numerical solution a representative case was calculated with an increasing number of mesh cells, N. The peak pressure at the target end is given in Table 2 for three cases: N=70,100 and 150. The variation of the peak overpressure at the target end was then plotted against $\delta=100/N$, where δ represents the cell size. Fig.12 shows the overpressure as function of δ^2. From this plot it is clear that the solution is converging linearly with δ^2 as the number of cells increases. The theoretical limit may be obtained by extrapolation to $\delta=0$. The limit value of the overpressure is 0.303. This value is about 22% over the N=70 calculation. In addition to the increase in the peak values, a measurable increase in the wave steepnes with N was also noticed, by inspection of the pressure time history for the three cases. (Not included in the paper).

In what follows, the computations will be carried out with a moderate value of N ($\approx$80) and then a "correction factor" will be applied to obtain the theoretical converged value.

TABLE 2
Peaks of the Normalized Overpressure as Function
of the Number of Mesh Cells in the Calculation

N	Peak	$\delta=100/N$	δ^2
70	0.2474	1.43	2.04
100	0.2768	1.00	1.00
150	0.2910	0.667	0.44

7. VARIABLE CROSS-SECTION RANGE

The final evaluation of the loads in the firing range were obtained with a variable cross-section model. In this quasi one-dimensional model the variation in cross-sectional area must be continuous. The actual discontinuous changes were therefore replaced by gradual variations of the area, as shown in Fig.13. The parameters of the problem were as follows: The propellant mass was taken as 9.8 Kg. In view of the discussion of section 7, Fc was taken as 0.1. Fp was taken as 0.30, (a more conservative value than indicated in [5]), and the specific propellant energy Q was taken as 4.6 MJ/Kg, according to the estimate of section 4. The number of computational cells was 80.

The pressure load time history at the target end is shown in Fig.14. The peak normalized overpressure is 0.19, with a pulse duration of about 100 ms. The first peak is immediately followed by a second peak of almost the same level, and a similar pulse duration. Both the peak level and pulse duration depend on the computational cell size. According to the analysis of section 6, the converged peak value should be about 20% higher, i.e. ~0.23. A further increase of the peak value by about 13% follows from the analysis of section 5, so that the estimate for the maximum load becomes ~0.26.

Another factor that affects the blast peak levels is the position of the muzzle within the range. The actual gun muzzle is located about 12.5m from the firing chamber end. However, the "center" of the muzzle blast may be a few meters away from the muzzle end, due to the motion of the combustion products. The nominal case quoted above assumed that the initial blast mixture occupied the space in the firing chamber between 12.5m to 14.5m from the chamber end. To assess the effect of the initial location of the muzzle blast, four cases were calculated, with varying position of the initial blast energy source. From the results of these calculations it was concluded that an additional factor should be applied to the peak load. This factor was estimated as ~1.17, which brings the load estimate from the former figure of 0.26 to ~0.30.

To sum up, the calculated loads should be amplified due to three effects: (a) numerical convergence (~20%), (b) kinetic energy of propellant gas (~13%), and (c) blast energy position (~17%).

An additional factor that could affect the load on the target end door is local two-dimensional flow, resulting from the geometry at the target end. This effect will be discussed in the next section.

8. TWO-DIMENSIONAL EFFECTS AT TARGET END

The flow at the target end requires special attention because the geometry deviates from the assumed cross-section uniformity. The shock wave which approaches the target end is almost planar, but the abrupt change in cross-section causes the wave to diffract. (Fig.15). The resulting curved shock propagates further into the target chamber, eventually reflecting from the walls. Although the diffraction weakens the shock, the subsequent reflections strengthen it, and it is difficult to estimate the net result without an appropriate two-dimensional calculation.

A two-dimensional calculation was carried out for the generic shape shown in Fig.15. The computational grid is shown in Fig.16. The flow was started assuming an oncoming plane shock front with a normalized peak overpressure of 0.15, decaying exponentially with time. The resulting flow field at selected times is shown in Figs.17. The velocity vector plot clearly show the diffraction of the wave and its interaction with the walls.

The pressure time histories at four locations are shown in Fig.18. The selected locations are indicated in Fig.15 by the numbers 2,4,5 and 6. Point 2 represents an almost undisturbed one-dimensional geometry. Points 4,5 and 6 represent typical positions at the target end door.

The curves indicate that peak pressure in excess of 0.3 are attained. The 0.3 level corresponds to ordinary reflection of a normal weak shock wave from a rigid wall. In fact the peak value at point 2 (Fig.18) is 0.29, as expected for this point, where the wave behaves locally as a plane wave. For the other locations, reflections contribute to higher peak values, about 0.35 for the three locations at the side wall with the door. (points 4,5 and 6). The two-dimensional effect for this case can be summed up by saying that an extra amplification of the peak occurs, from 0.3 to 0.35.

The calculated case is believed to be a conservative model of the actual geometry, and therefore the normalized peak overpressure of 0.35 should be considered an upper bound.

9. BLAST LOAD ON FIRING CHAMBER DOOR

The one-dimensional approach to the blast field within the proof range enables one to obtain cross-section averages of the flow variables. However, the averaged quantities are meaningful only at large distances from the energy source. The flow field in the vicinity of the muzzle is fully three dimensional, due to the complex wave reflections and refractions in the firing chamber. Nevertheless, an upper bound on the pressure load at the firing chamber door will be obtained, based on the one-dimensional model and known data on spherical blast waves from explosions.

The pressure time history at the door end predicted by the one-dimensional model is shown in Fig.20. The peak of the normalized overpressure is about 0.2, with a duration of about 40 ms. Applying a correction for numerical convergence brings the peak to ≈ 0.24. This figure constitutes the one-dimensional estimate.

An upper bound on the pressure peak may be obtained by taking the energy burst as a spherical explosion. The muzzle blast energy is equivalent to that of a 7 Kg TNT charge, assuming Fp=0.3. One finds for the normalized reflected overpressure from a 7 Kg charge at a distance of 12.5m a value of ≈ 0.47, using either tabulated data ([1], p.158) or the blast wave curves in well known manuals. This peak should be taken in conjunction with the load duration found from the one-dimensional model, despite the fact that the duration of the corresponding spherical blast would be much lower. It is believed that this definition of the load is on the safe side and thus a more elaborate two-dimensional calculation is not necessary.

10. VENTING FROM FIRING CHAMBER

It is well known that venting can alleviate the loads produced in closed structures by explosive blasts. However, the effectiveness of venting depends on the vent size and on the geometry of the structure.

The closed proof range has a large 5mx6m door at the end of the firing chamber. The effect of operating the range while this door is left open is examined in this section.

The computational model used for the closed end was modified at the firing chamber end (Fig.13). First, the cross-sectional area was reduced to the door opening. Second, the boundary condition at the end was modified to allow for the air to flow out of the opening, with an applied pressure equal to the ambient pressure. The resulting pressure time history at the target, Fig.21, is significantly different from the corresponding one for the closed end (Fig.14): It has only one significant peak as opposed to the double peaks in the closed end pressure pulse. The first peak is followed by a weak peak and a rather strong negative pressure. This negative phase is a result of the pressure rarefaction at the open end. However, from the practical view point the opening of the door does not reduce the design loads since the peak values are about the same, with a similar pulse duration.

11. SUMMARY AND CONCLUSIONS

The pressure loads inside a closed proof range resulting from the firing of a 155mm Howitzer (charge 10) were calculated using a computer code for unsteady compressible flow, and a simple model for the muzzle blast. It was found that the loading at the target end has a peak overpressure of the order of 0.35, with a pulse duration of over 100 ms. For the load at the firing chamber door, an upper bound on the peak of ~0.47 was estimated from data on spherical explosions, with a pulse duration of ~40 ms, based on the one-dimensional model.

Several factors that affect the calculated peak overpressure were discussed and estimated, namely:

- Effect of combustion products kinetic energy.
- Effect of numerical convergence.
- Effect of muzzle blast initial location.
- Two-dimensional effects of shock reflection at the target end.

The loads were found to have typical pulse duration of 40-100 ms. Since the loads are to be applied to structures having natural vibration periods of the same order of magnitude, the dynamic response of the structures must be considered.

L

REFERENCES

[1]   Baker, W.E.: "Explosions in Air", University of Texas Press, p.18-21 (1973).

[2]   Kivity, Y. and Feller, S.: "Blast Venting from a Cubicle", Proceedings of the 22nd DoD Explosives Safety Seminar, Anaheim, California, Aug. 1986.

[3]   Kivity, Y. and Kalkstein, A.: "Blast Wave Penetration into Cubicles". Proceedings of the 23rd DoD Explosives Safety Seminar, Atlanta, GA., Aug. 1988.

[4]   Gladstone, D.H. et al.,: "Studies of the Intermediate Ballistics of a Recoilless Rifle", Proceedings of the 7th Symposium on Ballistics, The Hague, The Netherlands, 1983.

[5]   Krier, H. and Adams, M.J., in "Interior Ballistics of Guns", Edited by Krier and Summerfield, p.9, Table 1 (1979).

[6]   Stiefel, L., in "Interior Ballistics of Guns", Edited by Krier and Summerfield, p.310, Table 2 (1979).

[7]   Heiney, K.O., in "Interior Ballistics of Guns", Edited by Krier and Summerfield, p.90, eq. 6, (1979).

[8]   Amsden, A.A., Ruppel, H.M., and Hirt, C.W.: "SALE : A Simplified ALE Computer Program for All Speeds", LA-8095 Report, Los Alamos National Lab. (1980).

[9]   Kivity, Y., and Golan, D.: "Response of an Imbedded Reactor Containment to Explosive Blast Loading", Proceedings of the 5th Confer. on Structural Mechanics in Reactor Technology, (SMIRT-5), Berlin, W. Germany (1979).

[10] Hancock, S.L.: "PISCES 2DELK Theoretical Manual", Physics International Company, San Leandro, CA. (1985).
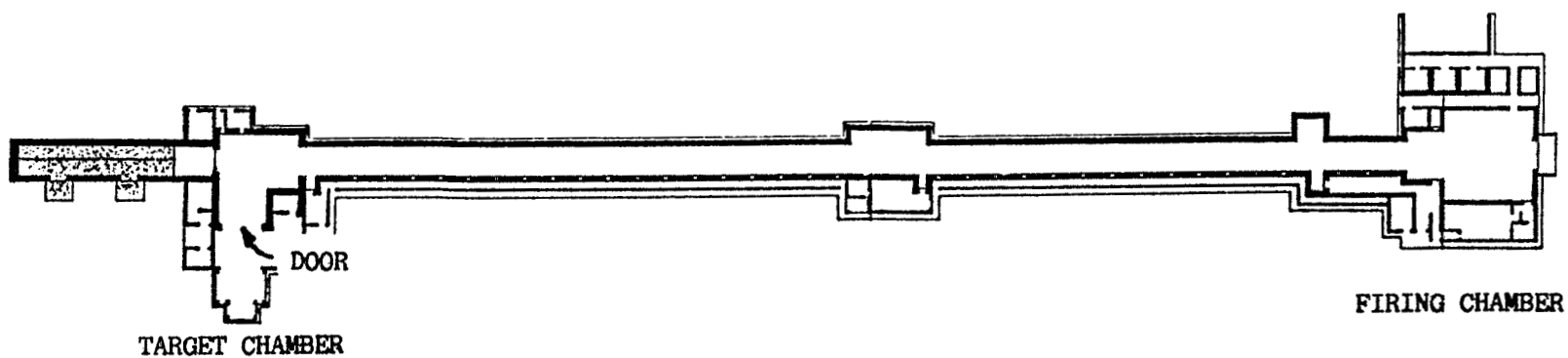
FIGURE 1a: SCHEMATIC OF THE FIRING RANGE
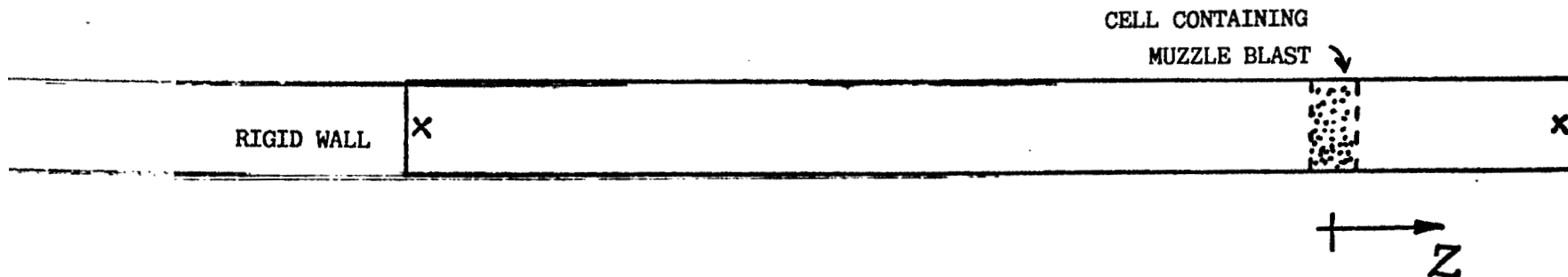
FIGURE 1b: THE COMPUTATIONAL MESH FOR THE
UNIFORM CROSS-SECTION RANGE.

X - LOCATION OF PRESSURE TIME HISTORY PLOT
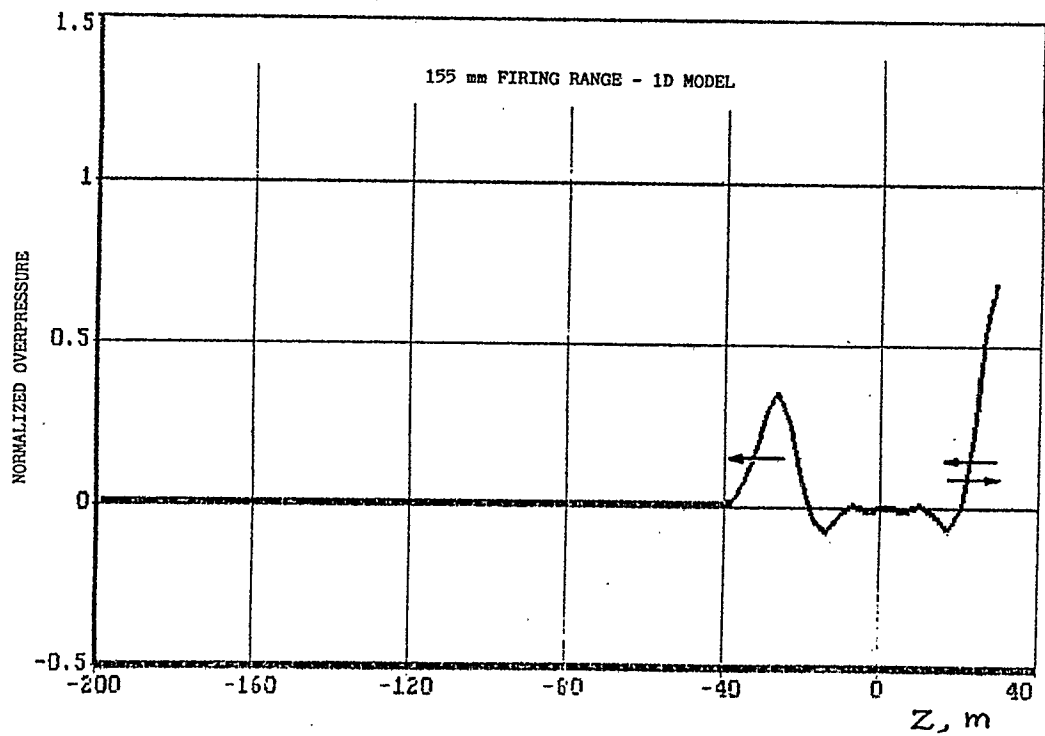
FIGURE 2: NORMALIZED OVERPRESSURE PROFILE AT TIME = 75 MS.
(UNIFORM CROSS-SECTION RANGE).
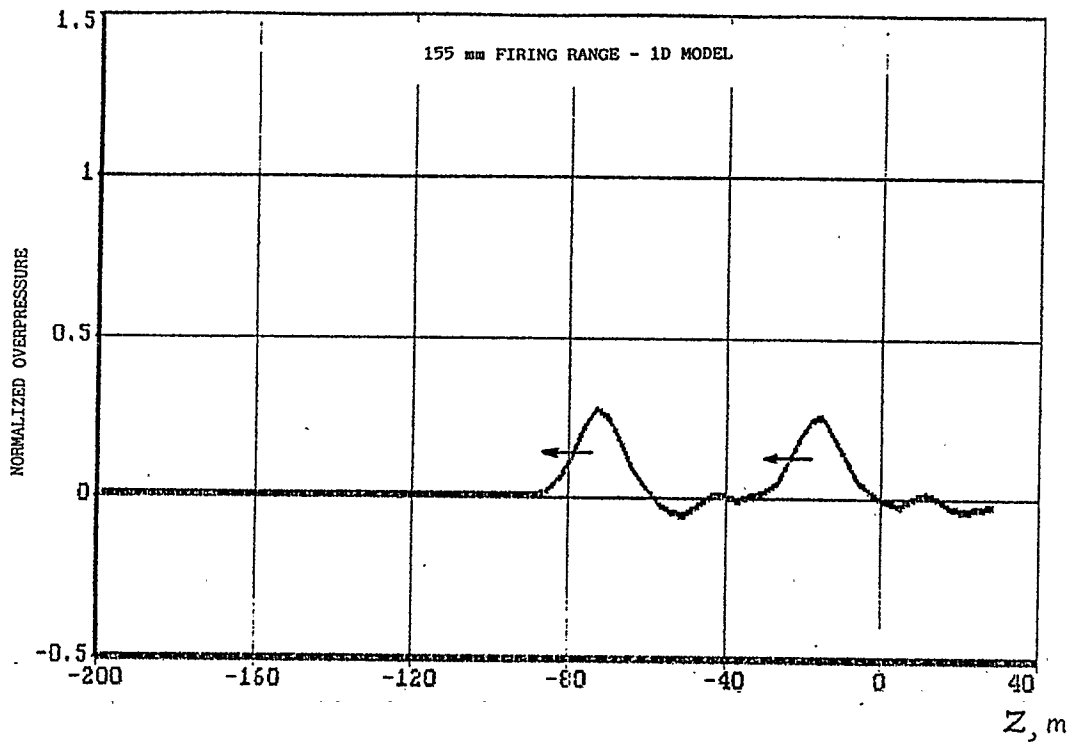
FIGURE 3: NORMALIZED OVERPRESSURE PROFILE AT TIME = 200 MS.
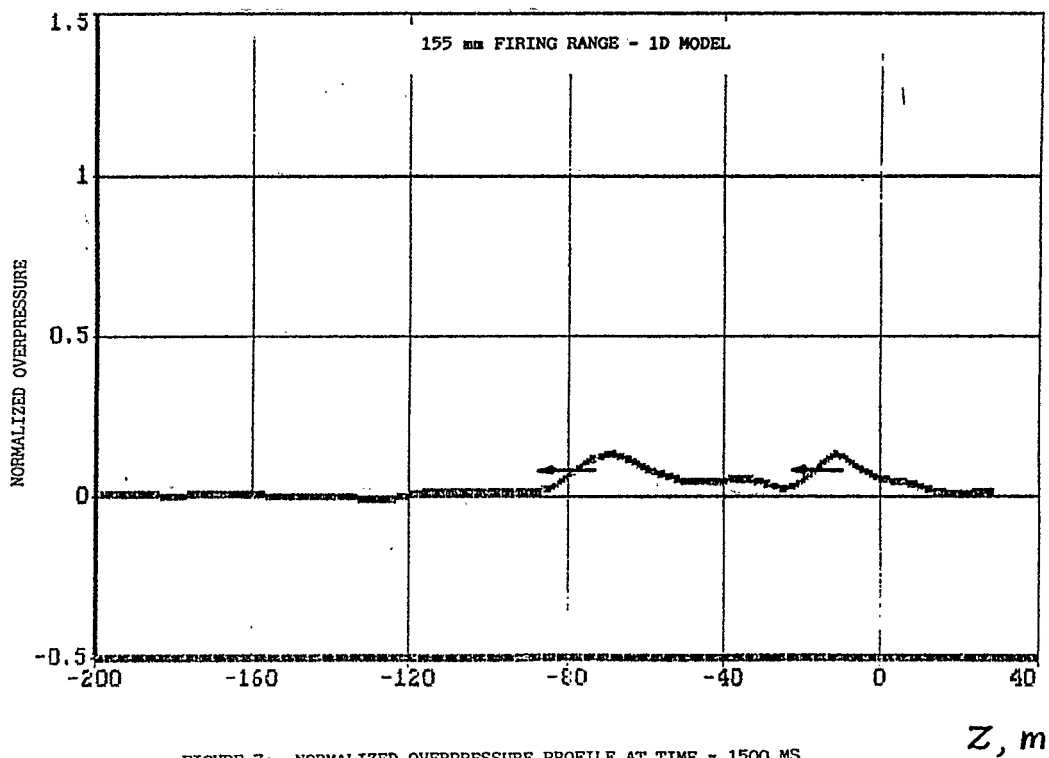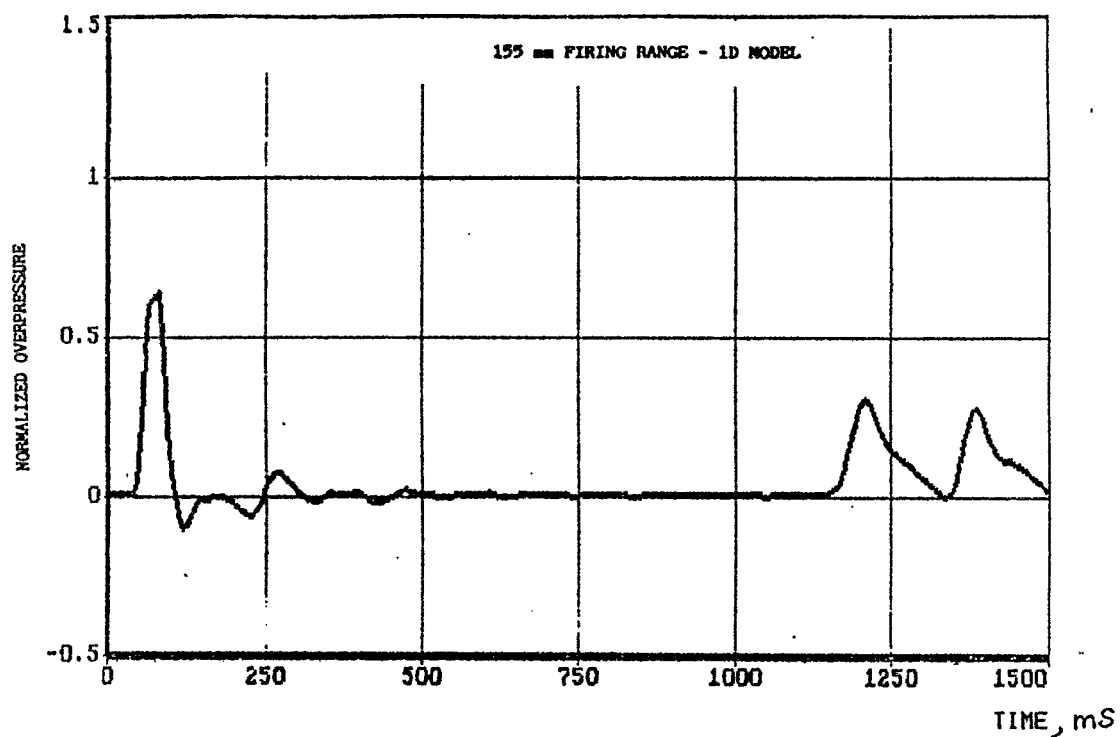(UNIFORM CROSS-SECTION RANGE).

773
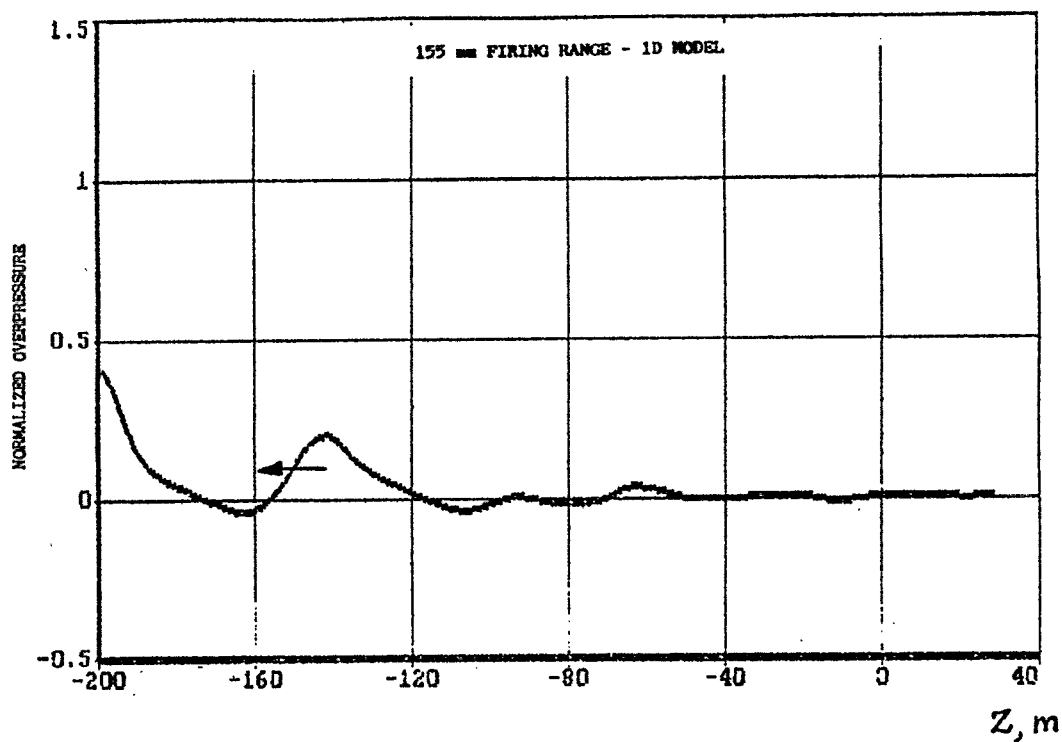
FIGURE 4: NORMALIZED OVERPRESSURE PROFILE AT TIME = 550 MS.
(UNIFORM CROSS-SECTION RANGE).
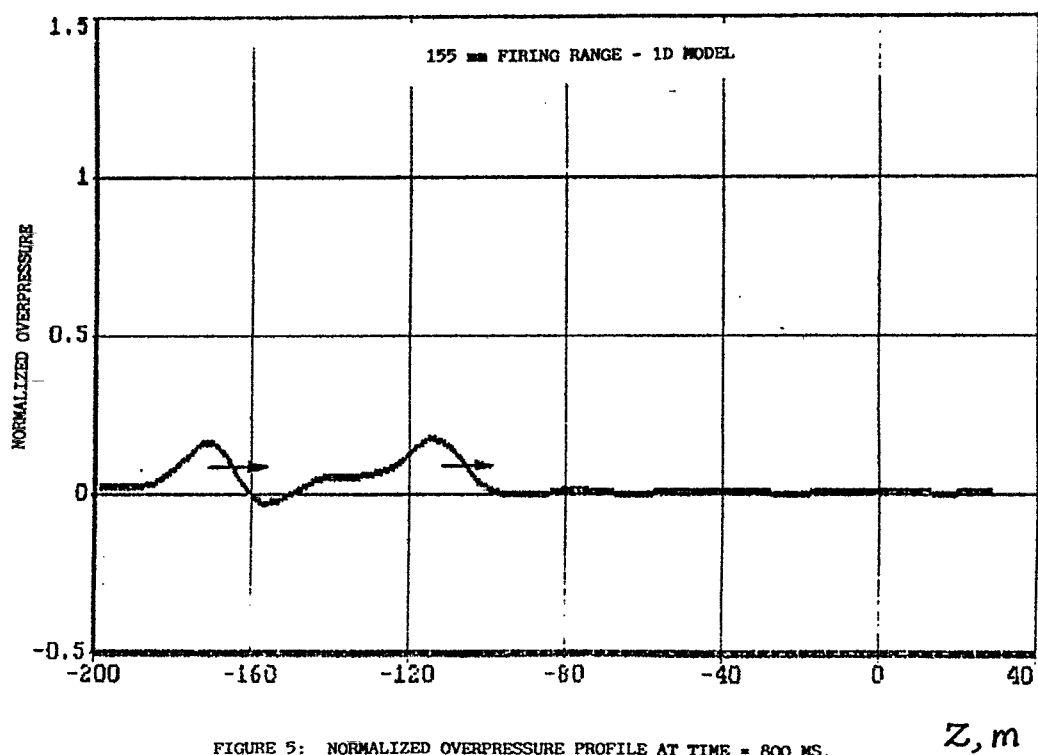
FIGURE 5: NORMALIZED OVERPRESSURE PROFILE AT TIME = 800 MS.
(UNIFORM CROSS-SECTION RANGE).
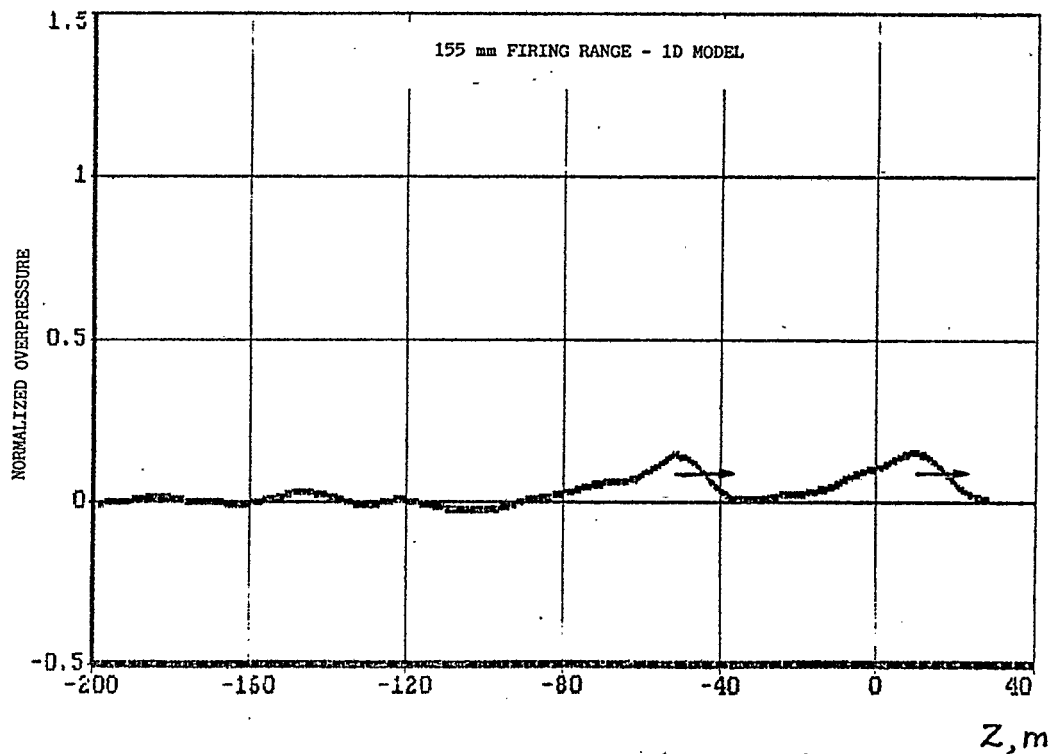
FIGURE 6: NORMALIZED OVERPRESSURE PROFILE AT TIME = 1150 MS.
(UNIFORM CROSS-SECTION RANGE).

FIGURE 7: NORMALIZED OVERPRESSURE PROFILE AT TIME = 1500 MS.
(UNIFORM CROSS-SECTION RANGE).

FIGURE 8:   PRESSURE TIME HISTORY AT THE FIRING CHAMBER END.
(UNIFORM CROSS-SECTION RANGE).
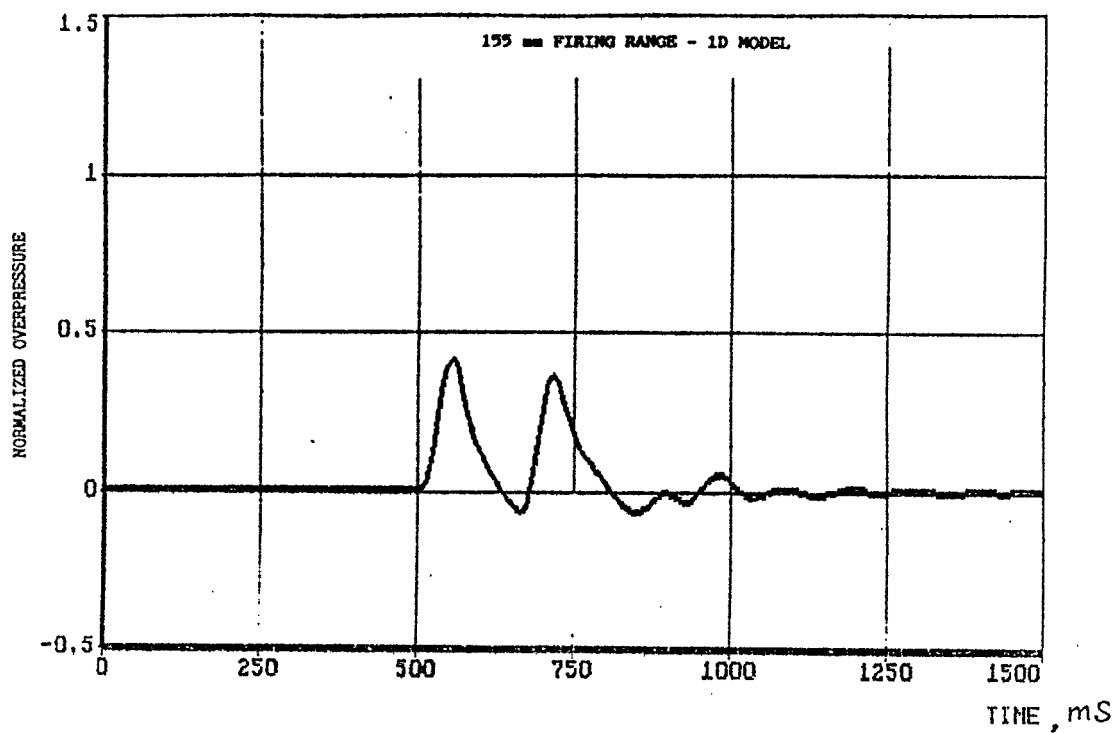
FIGURE 9 :   PRESSURE TIME HISTORY AT THE TARGET END (Z = -200).
(UNIFORM CROSS-SECTION RANGE).

FIGURE 10: PRESSURE TIME HISTORY AT THE TARGET END.
EFFECT OF PROPELLANT GAS KINETIC ENERGY.
Fp = 0.30 ; Fc = 0.

FIGURE 11: PRESSURE TIME HISTORY AT THE TARGET END.
EFFECT OF PROPELLANT GAS KINETIC ENERGY.
Fp = 0.30 ; Fc = 0.6

777
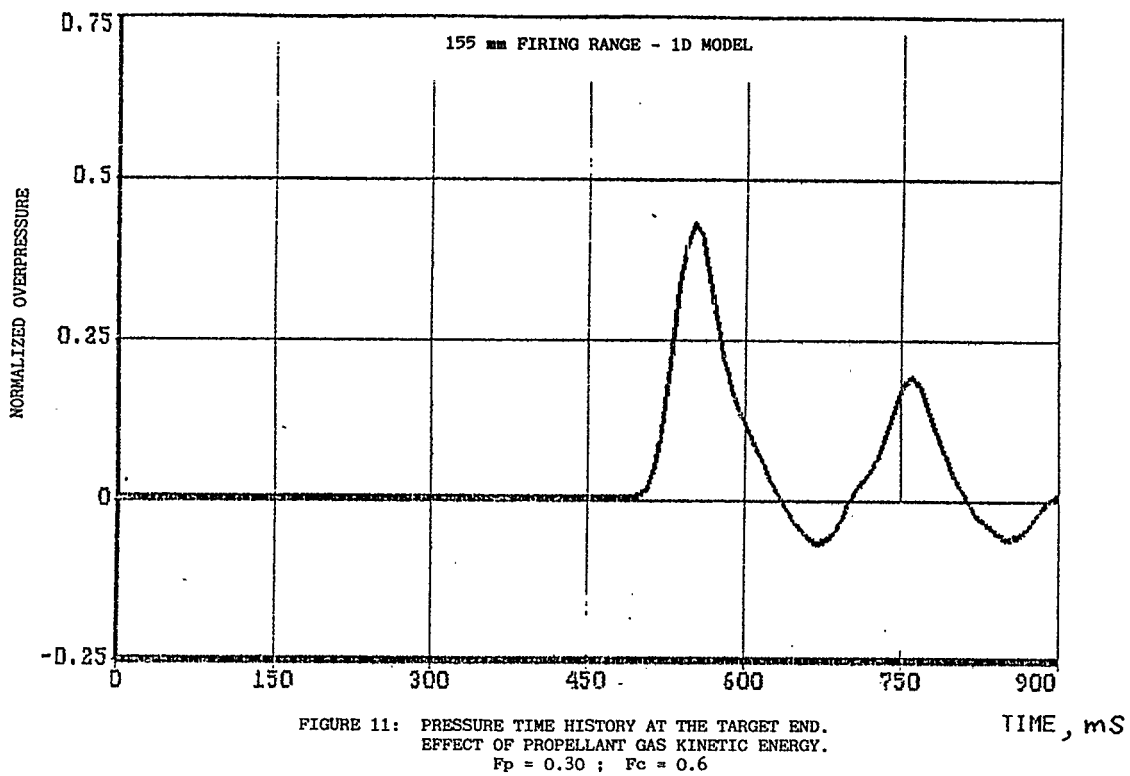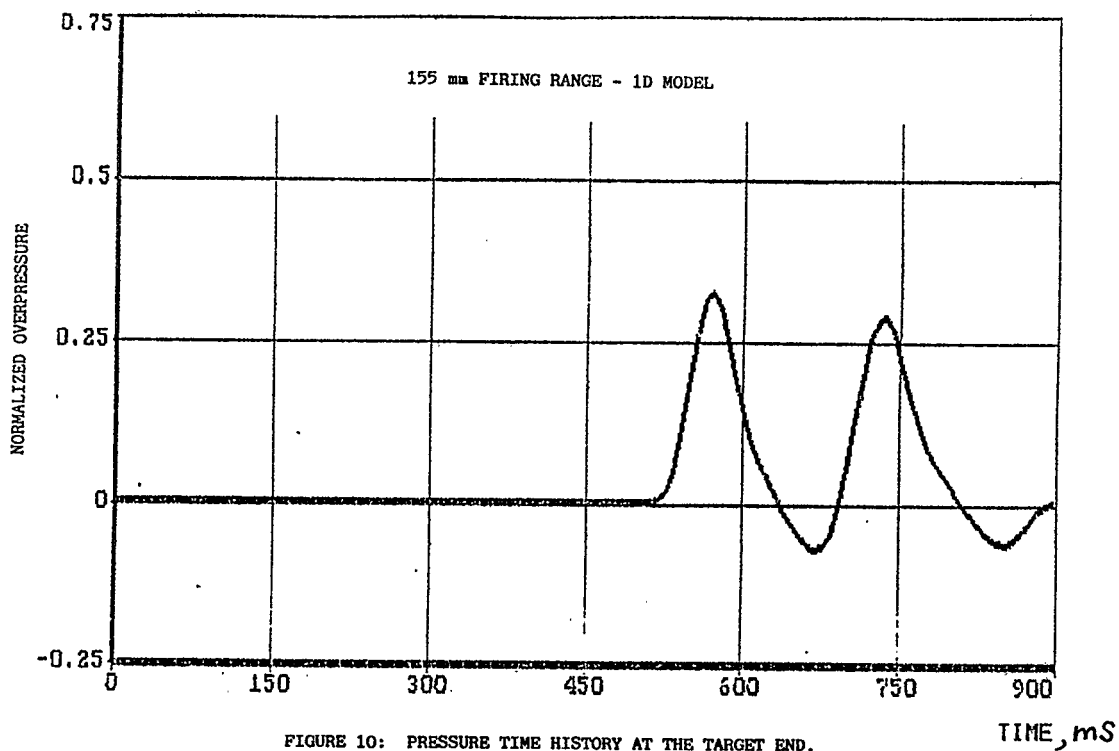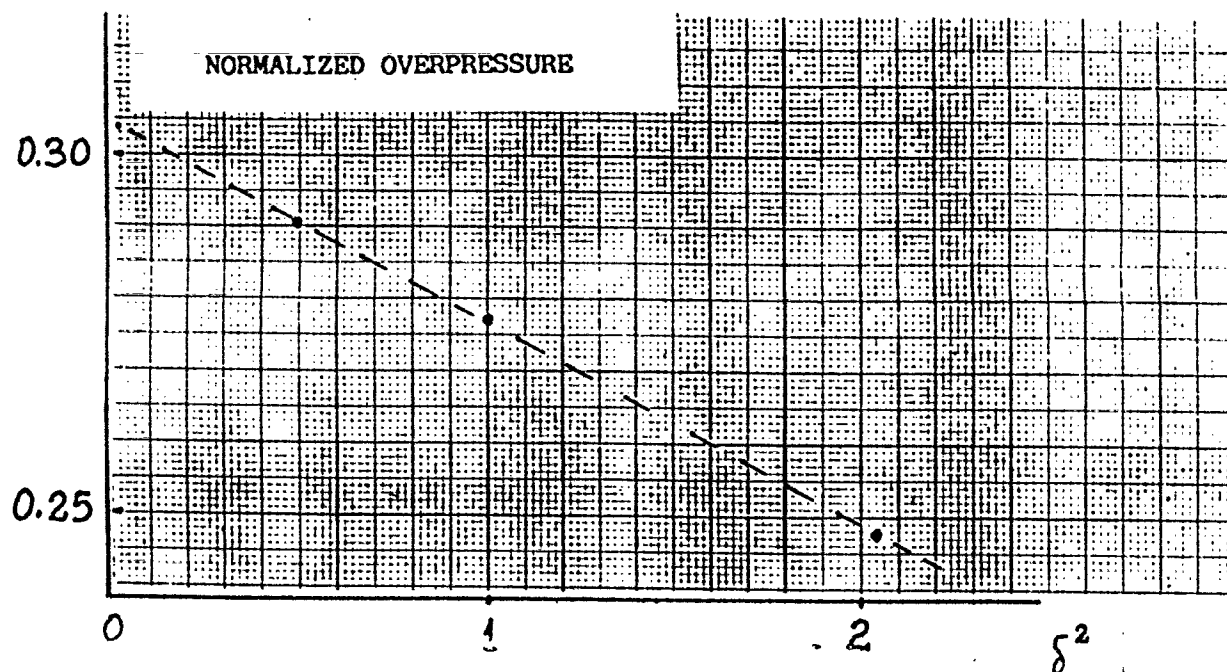
FIGURE 12: CONVERGENCE OF THE NUMERICAL SOLUTION.
N = NUMBER OF GRID CELLS; δ = 100/N.
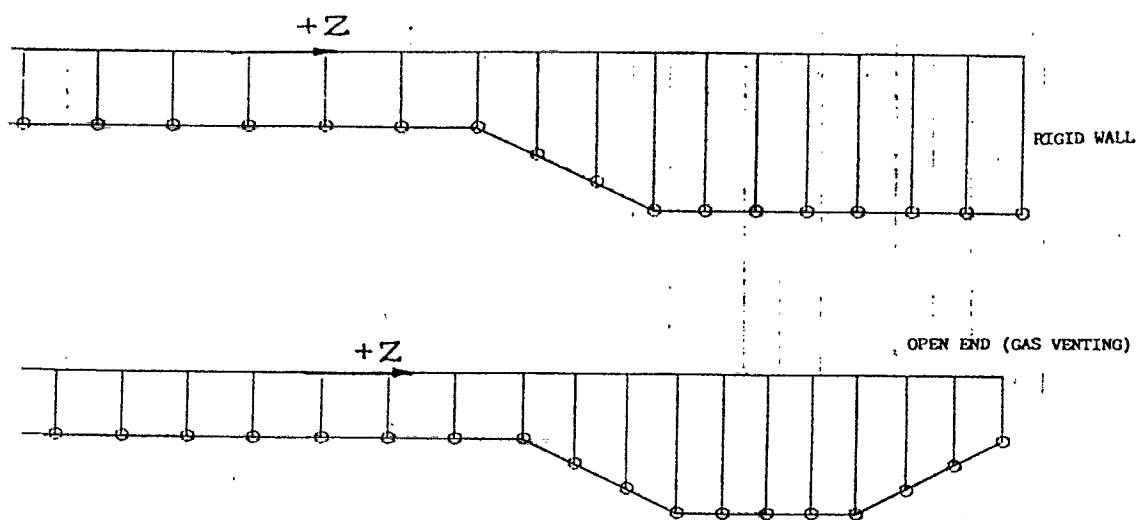
FIGURE 13: THE MESH FOR THE VARIABLE CROSS-SECTION RANGE.
TOP: FIRING CHAMBER DOOR CLOSED (NO VENTING).
BOTTOM: FIRING CHAMBER DOOR OPEN (WITH VENTING).
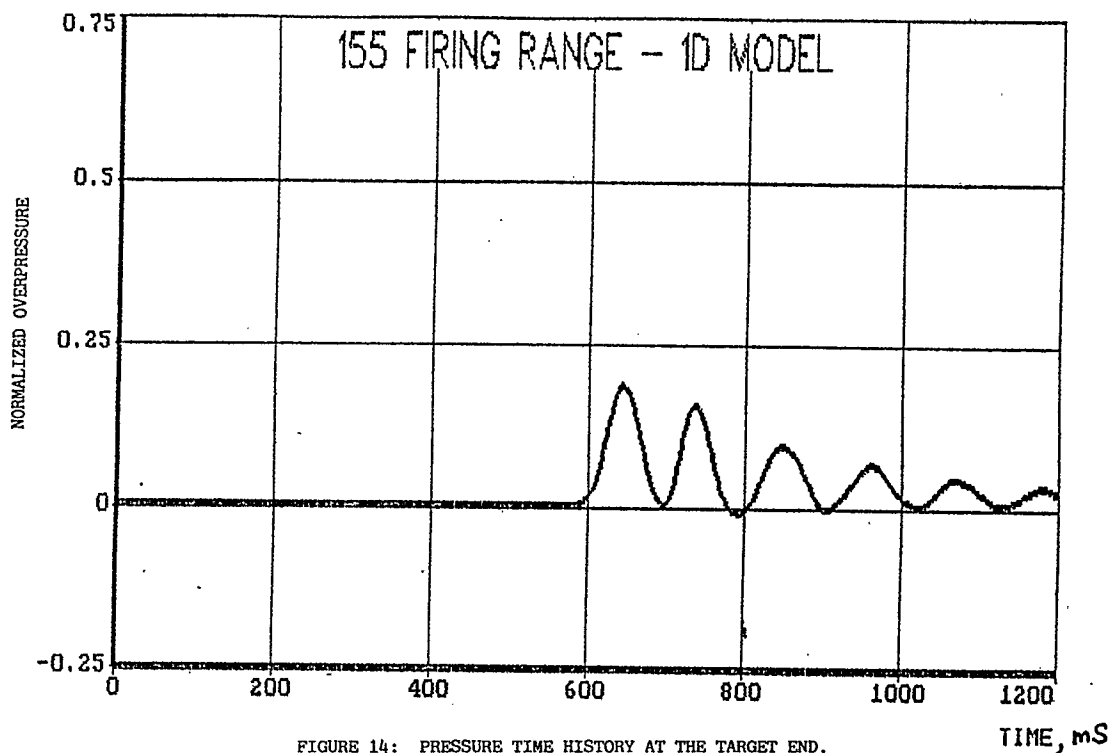
FIGURE 14: PRESSURE TIME HISTORY AT THE TARGET END.
VARIABLE CROSS-SECTION RANGE.
Fp = 0.30 ; Fc = 0.1
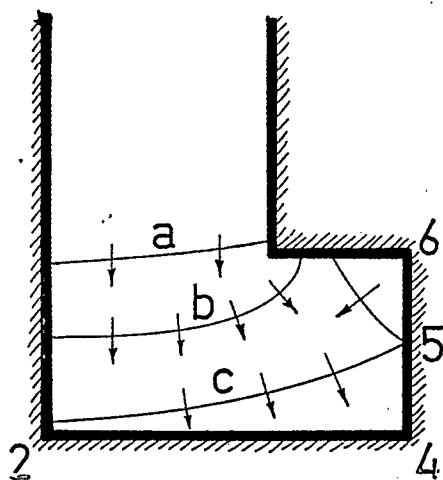
FIGURE 15: SCHEMATIC OF WAVE PROPAGATION
IN THE TARGET CHAMBER.

THE CURVED LINES INDICATE THE
SHOCK FRONT AT VARIOUS TIMES.
(TIME INCREASES FROM a TO c)
NUMBERS INDICATE LOCATIONS OF
PRESSURE TIME HISTORY PLOT.
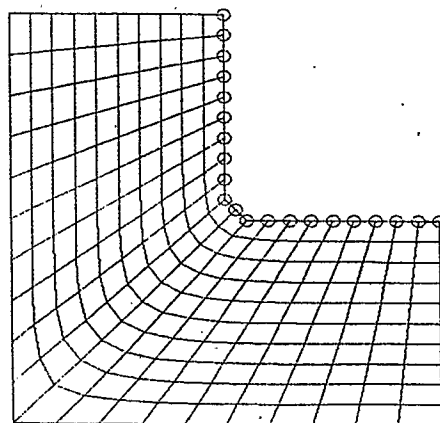
FIGURE 16: THE COMPUTATIONAL MESH FOR THE
TWO-DIMENSIONAL CALCULATION.
(TARGET END SIMULATION).
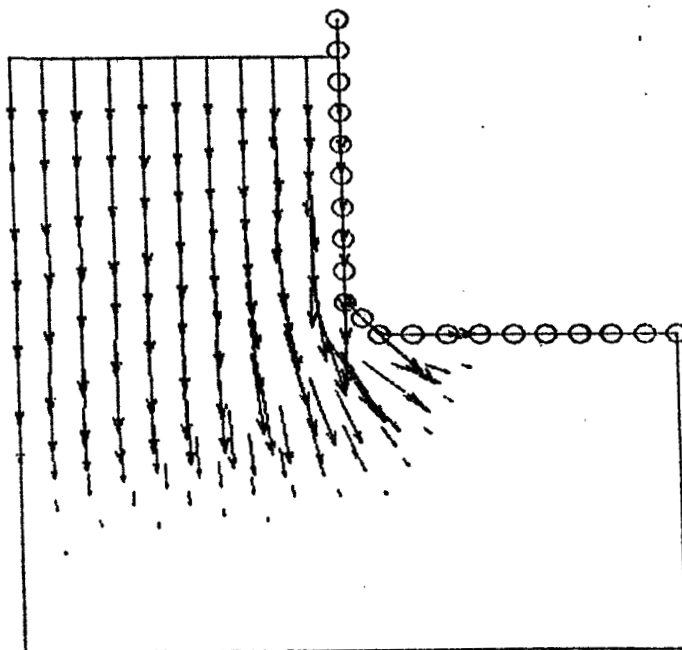
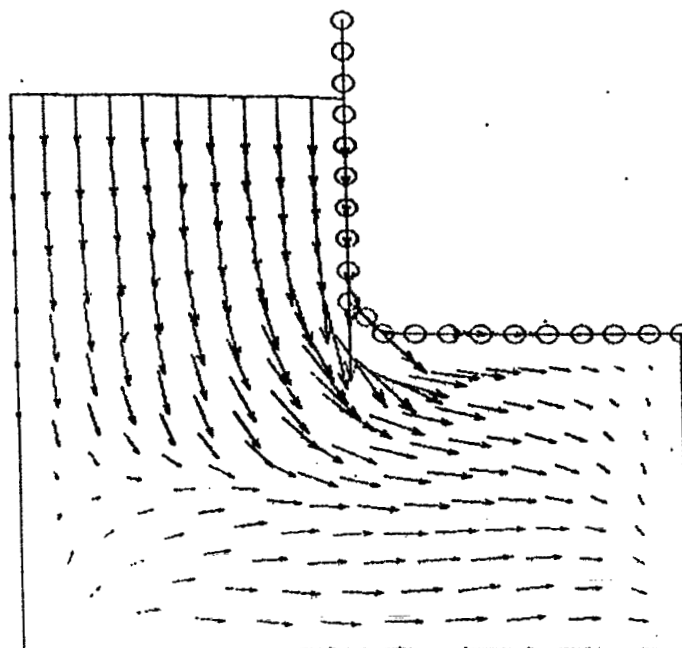FIGURE 17a: VELOCITY VECTOR PLOT AT TIME=20 MS.
(TARGET END SIMULATION).

FIGURE 17b: VELOCITY VECTOR PLOT AT TIME=40 MS.
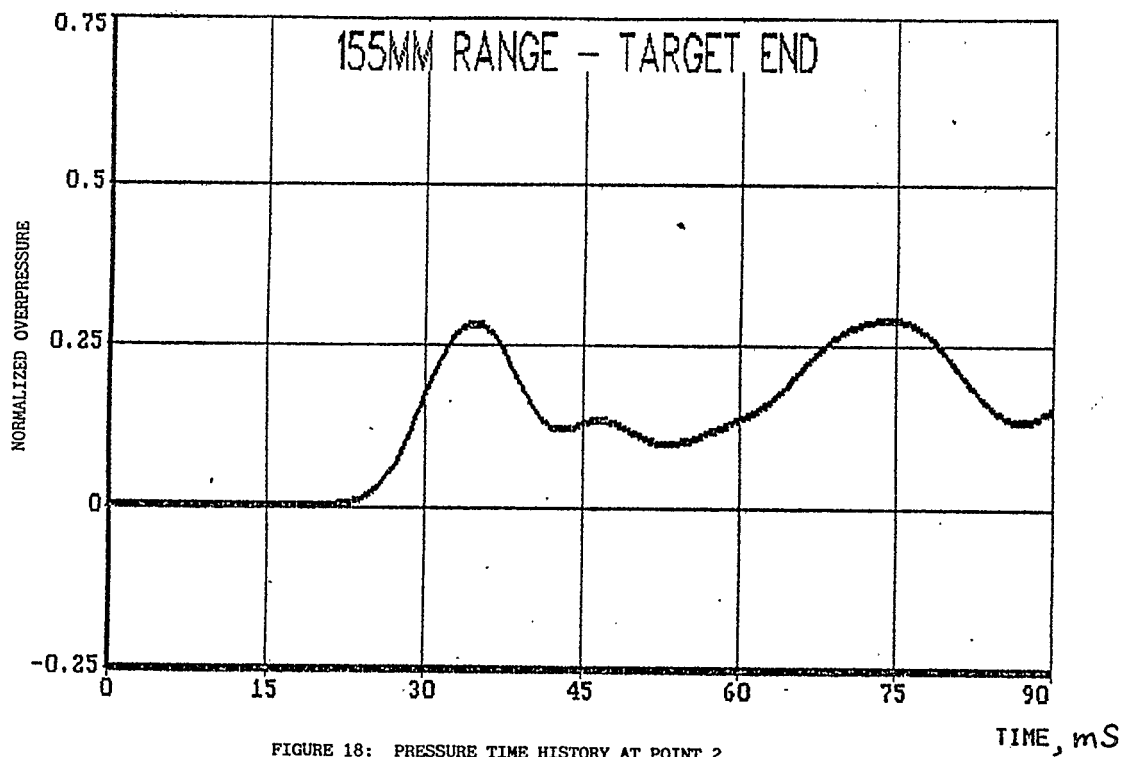(TARGET END SIMULATION).

FIGURE 18:   PRESSURE TIME HISTORY AT POINT 2
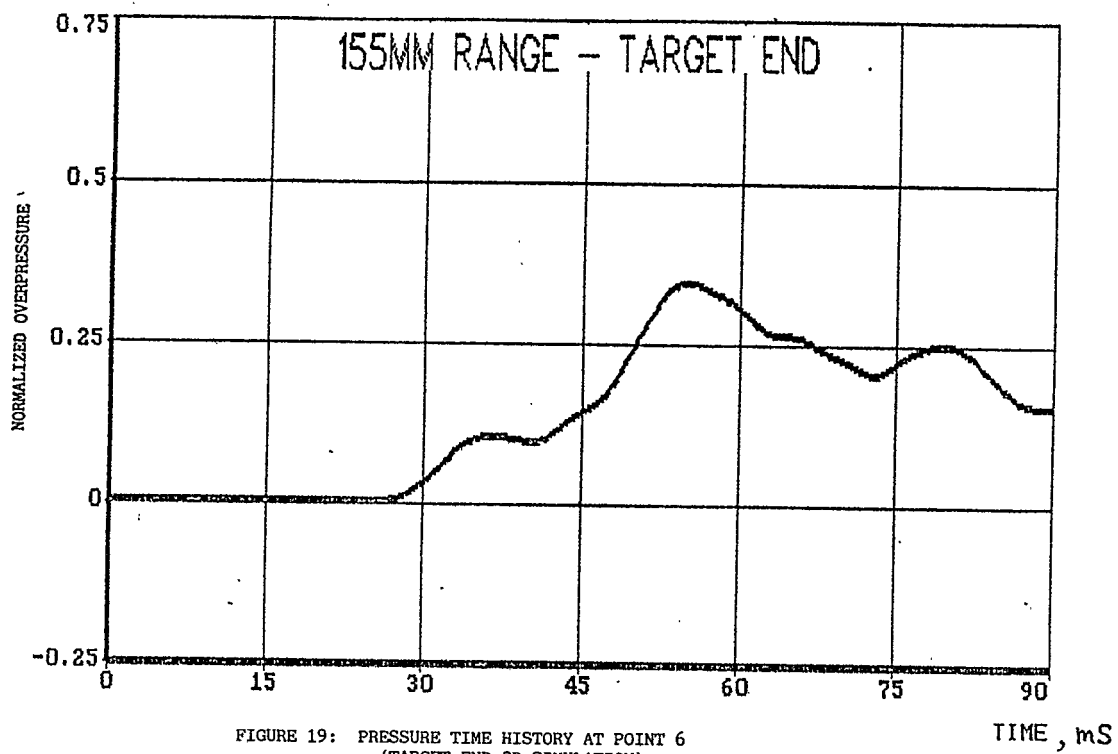(TARGET END 2D SIMULATION)

FIGURE 19:   PRESSURE TIME HISTORY AT POINT 6
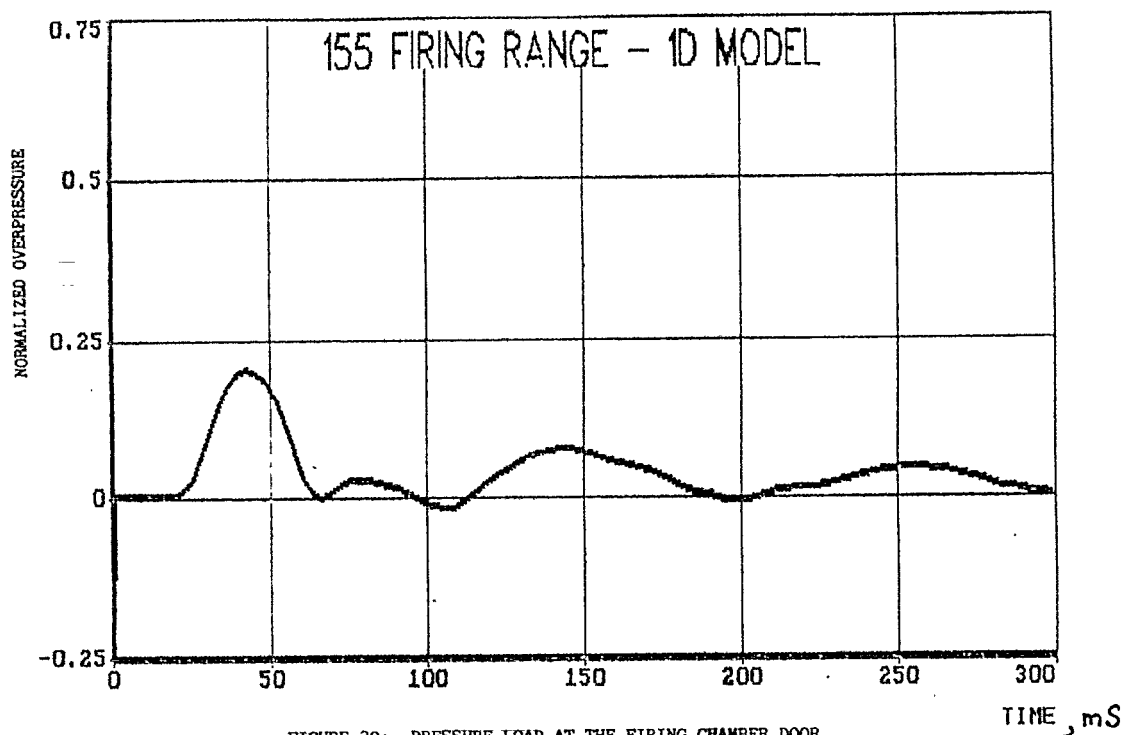(TARGET END 2D SIMULATION)

FIGURE 20: PRESSURE LOAD AT THE FIRING CHAMBER DOOR.
VARIABLE CROSS-SECTION RANGE.
Fp = 0.30 ; Fc = 0.0

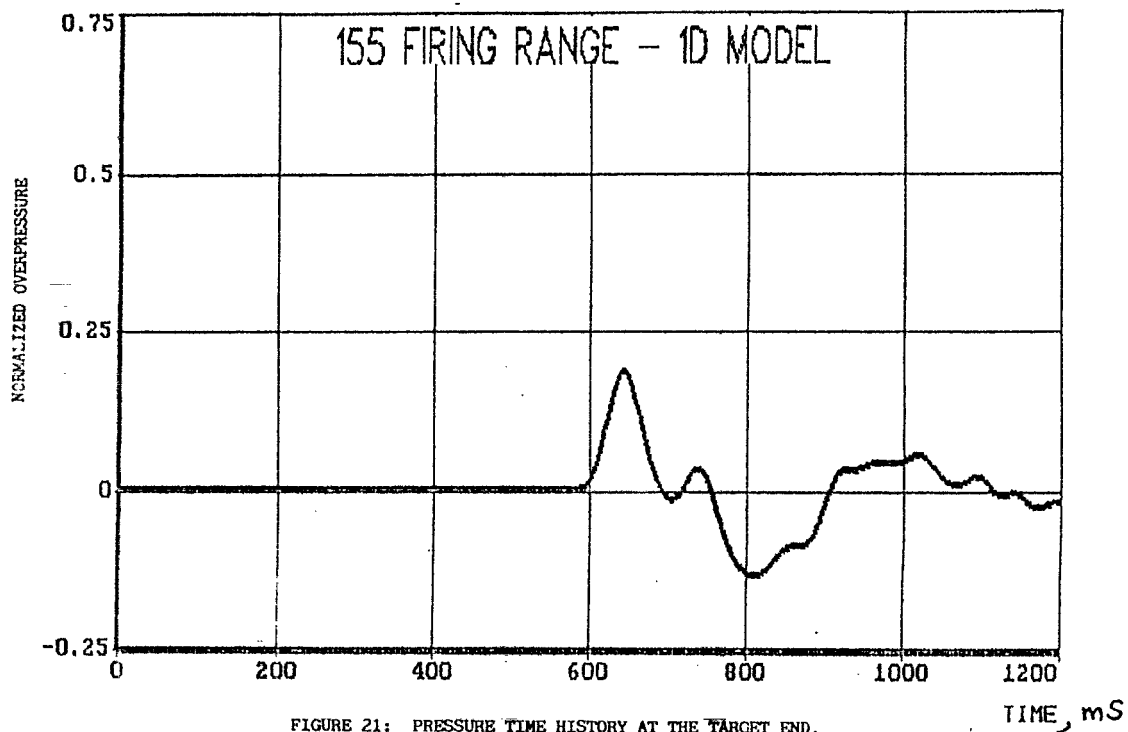FIGURE 21: PRESSURE TIME HISTORY AT THE TARGET END.
VARIABLE CROSS-SECTION RANGE, WITH VENTING.
Fp = 0.30 ; Fc = 0.1